

Supplementary Information

Exploring Vinyl Polymers as Soft Carbon Precursors for M-ion (M = Na, Li) Batteries and Hybrid Capacitors

Afshin Pendashteh, Brahim Orayech, Jon Ajuria, María Jáuregui, and Damien Saurel *

Centre for Cooperative Research on Alternative Energies (CIC energiGUNE), Basque Research and Technology Alliance (BRTA), Alava Technology Park, Albert Einstein 48, 01510 Vitoria-Gasteiz, Spain.

* Correspondence: dsaurel@cicenergigune.com

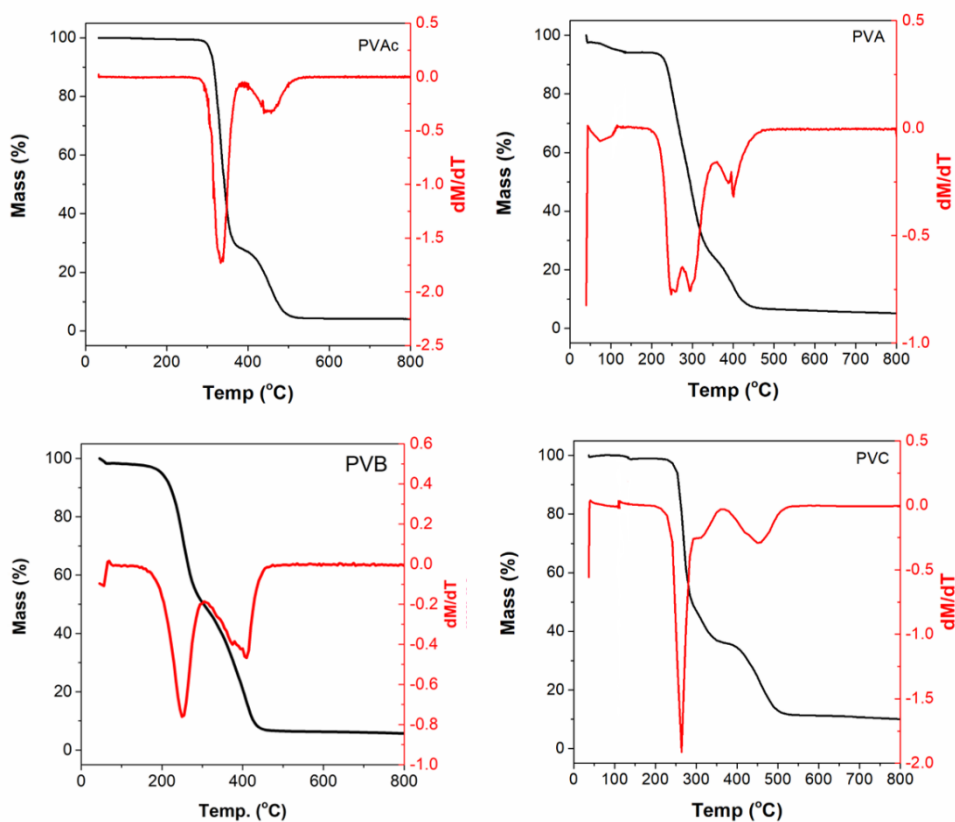


Figure S1. Thermo-gravimetrical analysis of the vinyl polymers under Ar atmosphere.

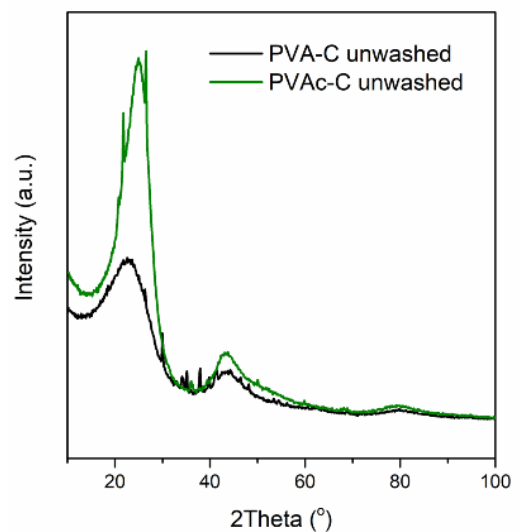


Figure S2. PXRD patterns of PVA- and PVAc-C samples before rinsing with water and ethanol.

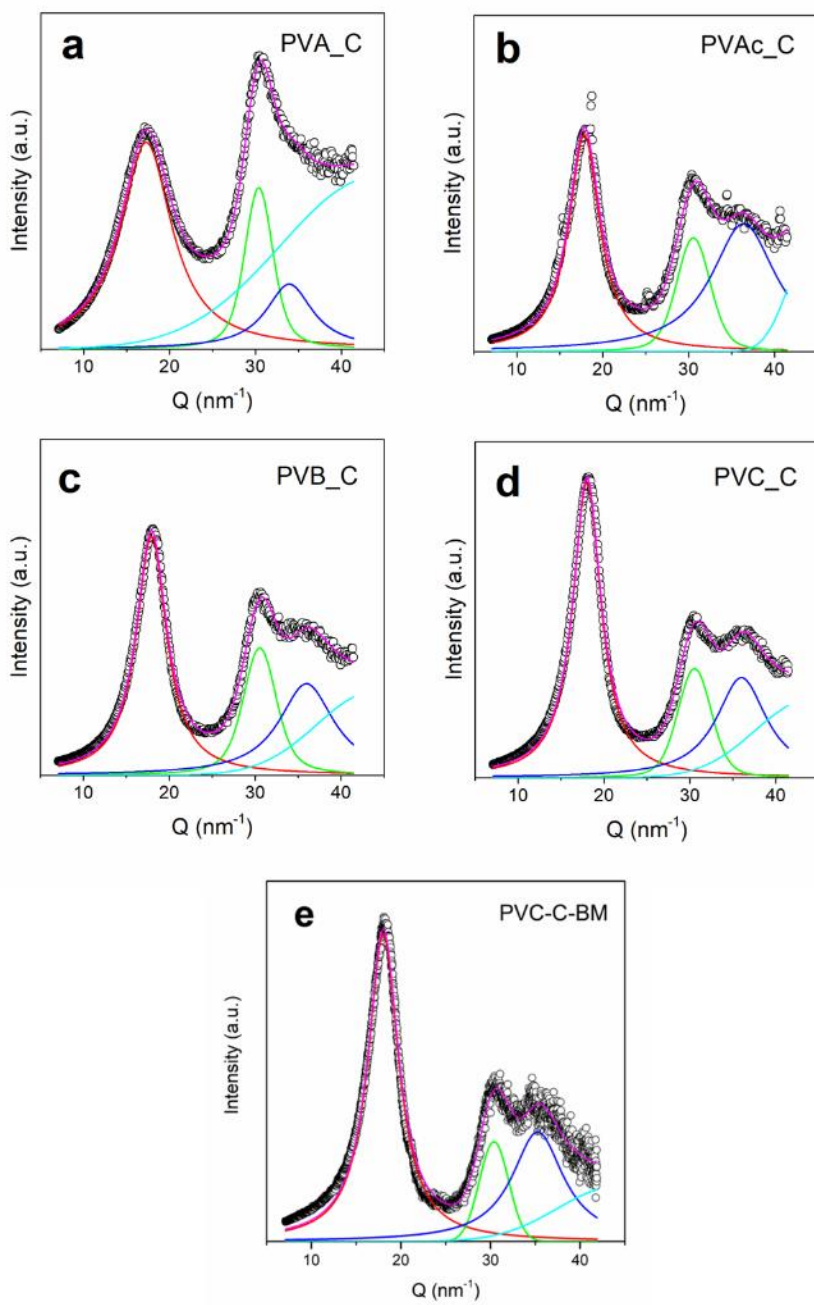


Figure S3. Corrected PXRD patterns of the pyrolyzed polymers as well as the ball-milled PVC-derived SC (PVC-C-BM) for polarization, Lorentz, and illuminated sample volume factors along with the fitting results with Voigt peaks.

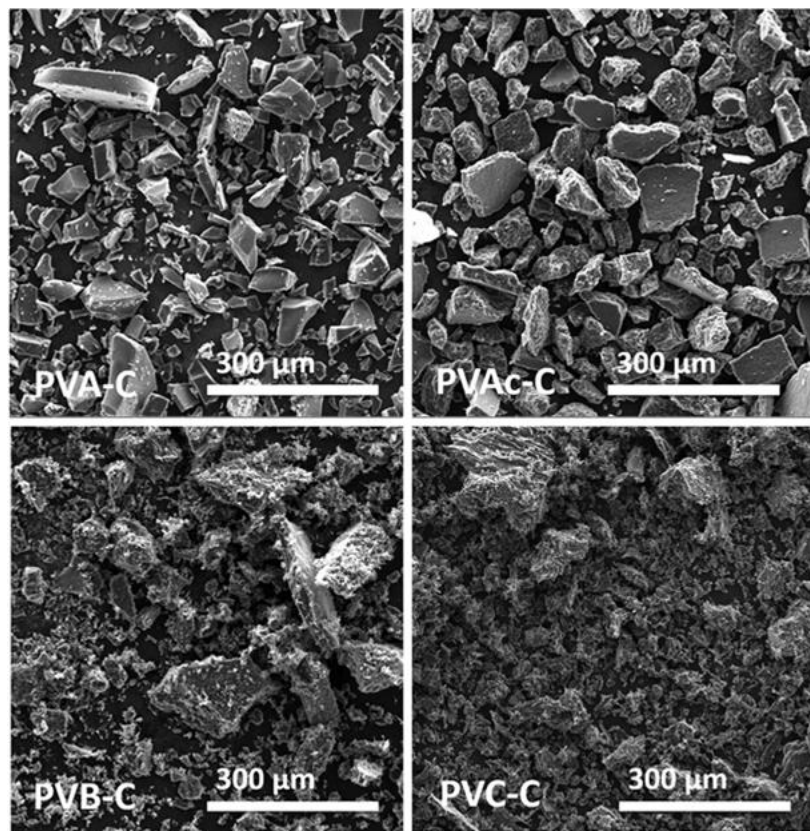


Figure S4. Scanning electron micrographs of the vinyl polymer-derived carbons at a pyrolysis temperature of 800 °C under Ar atmosphere, in a magnification of 300x.

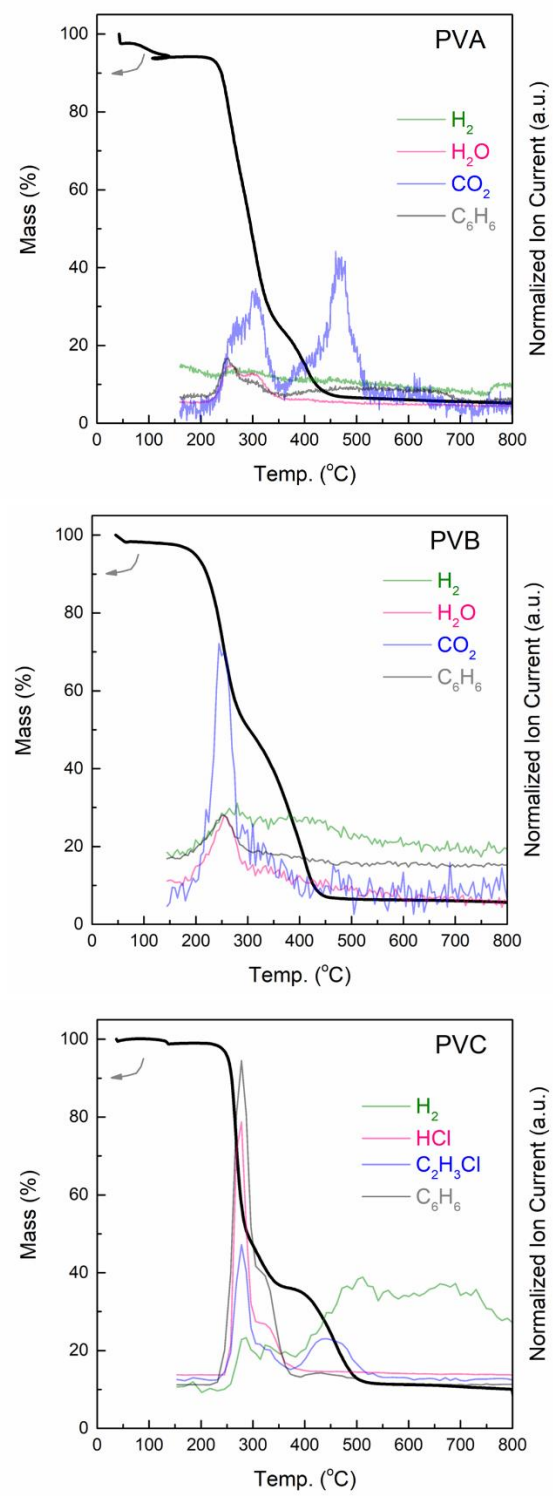


Figure S5. TG profiles of the samples along with their residual gas analysis.

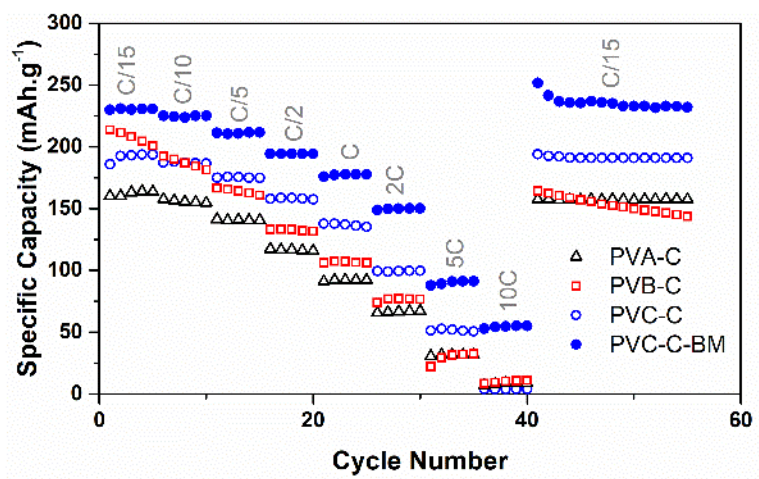


Figure S6. Rate capability (based on Q_{rev}) of the polyvinyl-derived soft carbons at various current loads ranging from C/15 to 10C.

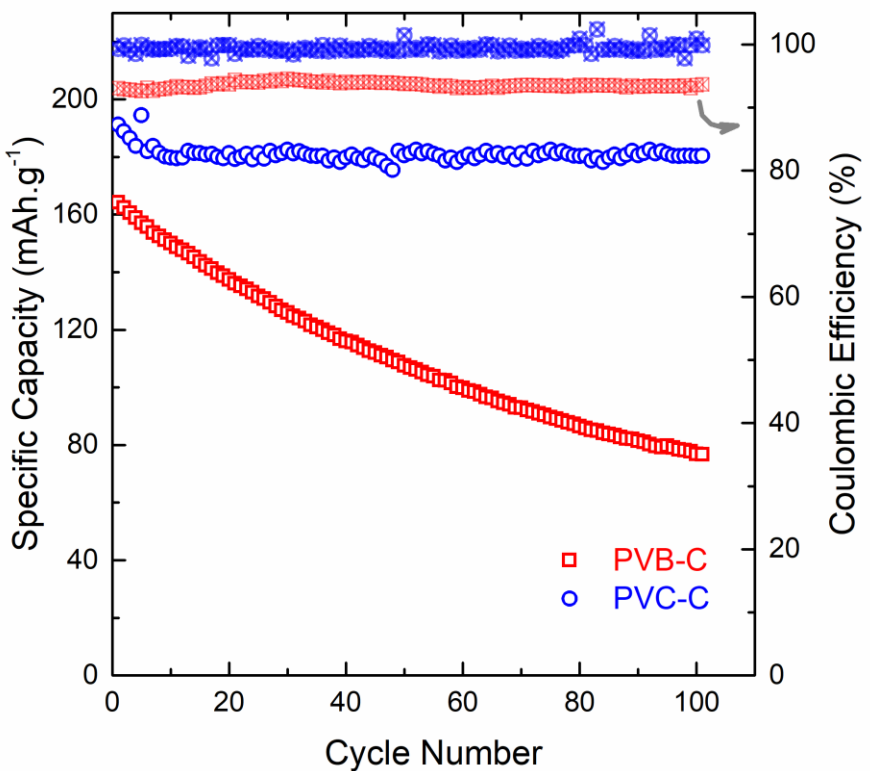


Figure S7. Cycling performance of the PVB-C and PVC-C samples in half cell vs Na at a current load of C/15 along with their coulombic efficiency.

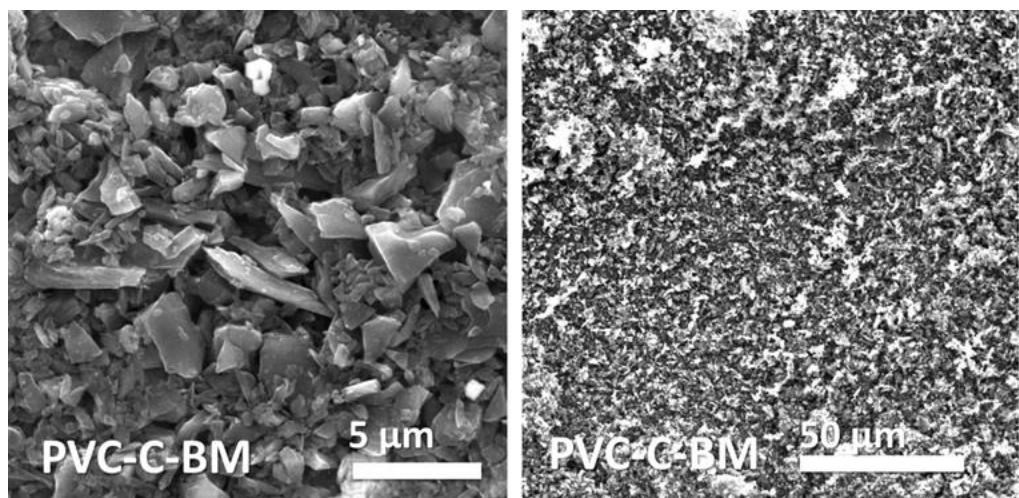


Figure S8. SEM images of the ball-milled PVC-derived carbon (PVC-C-BM).

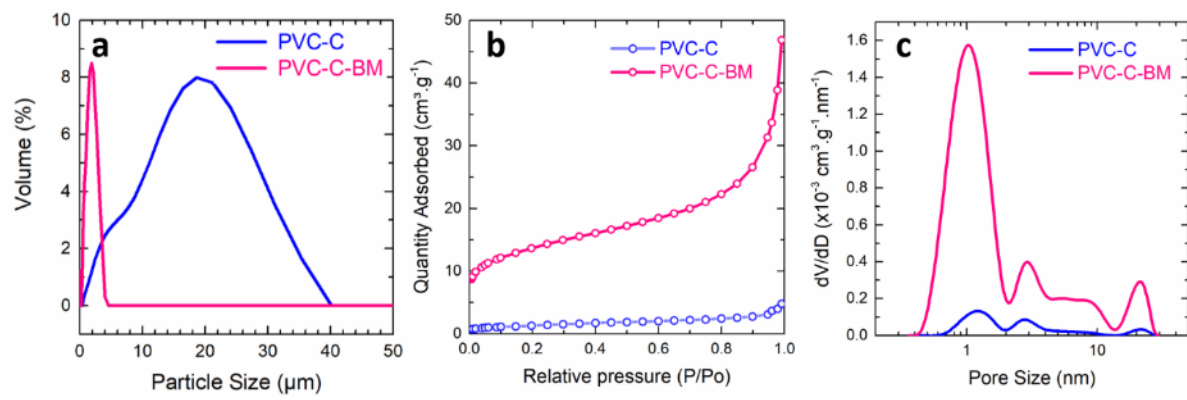


Figure S9. Particle size distribution (a), N_2 adsorption isotherms (b); and pore size distribution based on NLDFT (Non-Local Density Functional Theory) of the PVC-derived soft carbons (pristine: PVC-C and ball-milled: PVC-C-BM).

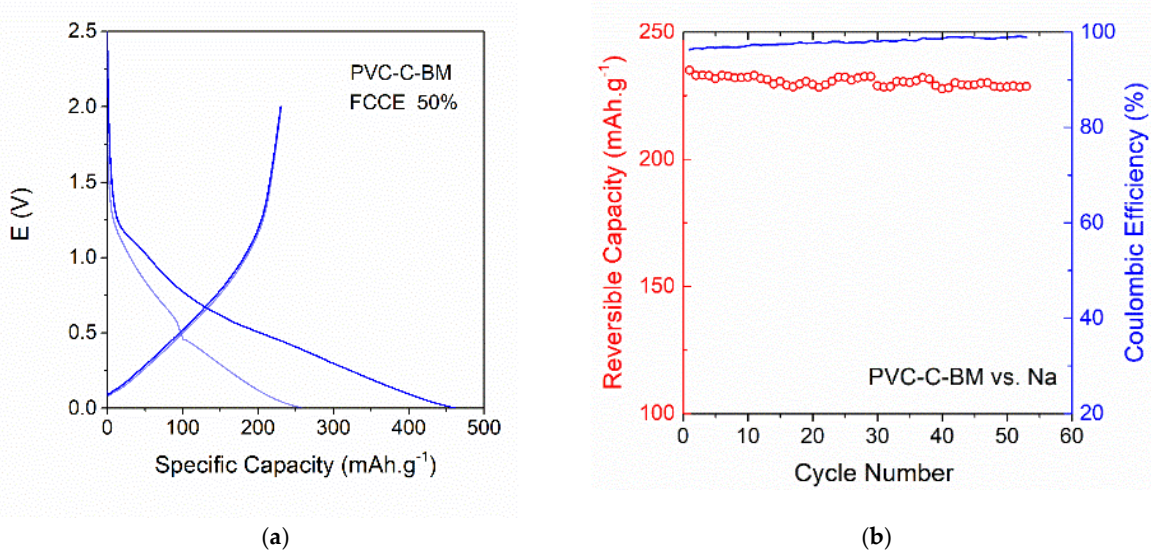


Figure S10. Sodium storage properties of the PVC-C-BM sample: (a) Two first discharge-charge cycles and (b) cycling performance of the PVC-C-BM sample in 1 M NaClO_4 in EC:PC at C/15 rate.

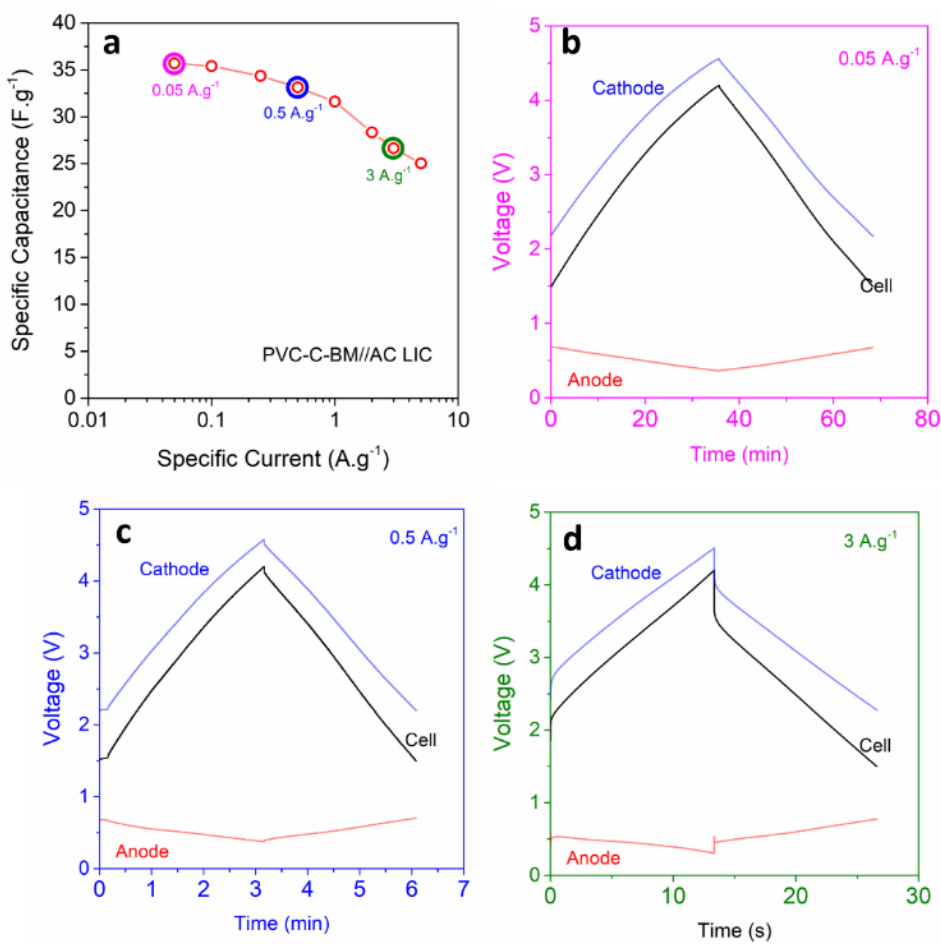


Figure S11. Electrochemical performance of the PVC-C-BM sample as the negative electrode in integration with YP80F Activated Carbon in hybrid lithium capacitors in mass ratio of SC:AC of 2:1: (a) rate capability of the PVC-C-BM//AC LIC device in 1 M LiPF₆ in EC:DMC; and the real time profiles of the hybrid cell in (b) 0.05 $\text{A}\cdot\text{g}^{-1}$, (c) 0.5 $\text{A}\cdot\text{g}^{-1}$, and (d) 3 $\text{A}\cdot\text{g}^{-1}$.

Table S1. The obtained properties of the SCs derived from pyrolysis of vinyl polymers.

Sample	Pyrolysis Yield (%)	Yield _{TG} (%)
PVA-C	5.70(4.63) ¹	5.15
PVAc-C	4.98(3.8)	4.10
PVB-C	7.6	5.67
PVC-C	11.0	10.0

¹ The yield in parenthesis was obtained after rinsing with water and ethanol.

Table S2. Comparison of the electrochemical performance of the previously reported soft carbons at low rate (at $\leq 40 \text{ mA}\cdot\text{g}^{-1}$, except (*) at $100 \text{ mA}\cdot\text{g}^{-1}$). When not mentioned in the original report, the average oxidation potential, $\langle E_{\text{ox}} \rangle$, the reversible specific capacity (C_{re}) and/or the first cycle Coulombic efficiency (FCCE), were estimated by digitalization of the reported voltage–composition curves. Equation S1 was employed to estimate the full cell specific energy, considering the *Faradion* layered oxide as cathode material (165 $\text{mAh}\cdot\text{g}^{-1}$ at 3.2 V).

Precursor	Pyrolysis Temp. (°C)	$\langle E_{\text{ox}} \rangle$ (V)	C_{re} (mAh·g ⁻¹)	FCCE (%)	Energy (Wh·kg ⁻¹)	Ref.
PVA-C	800	0.498	160	65	219	This Study
PVB-C	800	0.529	212	56	248	This Study
PVC-C	800	0.547	195	70	237	This Study
PVC-C-BM	800	0.656	249	54	252	This Study
Petroleum Coke (PeC)	NA	-	70	-	--	1993 [1]
Carbon Black (Sawinigan)	NA	-	132	-	--	1993 [1]
Carbon Black (YPF)	NA	0.827	89	21	137	2001 [2]
Carbon Black (YPF)	NA	0.677	121	29	176	2001 [2]
Acetylene Black	NA	0.476	77	20	143	2001 [2]
Carbon Black (Super P)	NA	0.550	152	40.4	209	2014 [3]
Mesophase Pitch	NA	0.670	120	20	176	2011 [4]
PTCDA ¹	700	0.565	230	62	253	2015 [5]
PTCDA	900	0.479	200	66	246	2015 [5]
PTCDA	1100	0.430	125	65	197	2015 [5]
PTCDA	1600	0.468	90	47	159	2015 [5]
PTCDA	900	0.602	184	80	226	2017 [6]
PTCDA	900	0.501	200	67	244	2017 [7]
Mesitylene	700	0.490	130	60	197	2014 [8]
NTCDA ²	500	1.210	125	46	141	2015 [9]
PVC ³	600	0.494	199	65.4	244	2000 [10]
PVC	700	0.481	211	65.5	252	2000 [10]
PVC	800	0.445	212	65.8	256	2000 [10]
PVC	900	0.448	167	69.1	229	2000 [10]
PVC	1000	0.406	148	68.9	218	2000 [10]
PVC	1100	0.349	126	59.3	204	2000 [10]
PVC	1200	0.346	116	61.6	194	2000 [10]
PVC	1300	0.346	92	57.1	168	2000 [10]
PVC	1400	0.324	91	47.1	168	2000 [10]
PVC	1700	0.329	71	54.1	143	2000 [10]
PVC	600	0.508	200	66.3	243	2001 [11]
PVC (fiber)	700	0.573	271	70	269	2015 [12]
Polystyrene/D-glucose	1000	0.850	220	70	221	2012 [13]
PEO/PPO tri-block copolymer	500	0.950	234	71	218	2016 [14]
Pitch	600	0.442	164	56.4	227	2000 [10]
Pitch	800	0.547	174	64.7	225	2000 [10]
Pitch	1000	0.417	146	59.4	215	2000 [10]
Pitch	1200	0.396	114	55.2	189	2000 [10]
Pitch	1000	0.391	150	69.2	220	2001 [11]
Mesophase pitch /MCMB ⁴	750	0.568	166	44.2	217	2000 [15]
Mesophase pitch /MCMB	700	0.610	240	66	253	2015 [16]
Mesophase pitch - templated	800	0.656	244	71	250	2016 [17]
Mesophase pitch - templated	800	1.130	331	45	228	2016 [17]
Petroleum Coke (PeC)	800	0.535	120	37	185	2002 [18]
Cellulose nano-crystals (CNC)	1000	1.430	450	25	214	2017 [19]
Polymerized acetone	800	1.310	359	34	214	2015 [20]

1) PTCDA: Perylenetetracarboxylic dianhydride; 2) NTCDA: Naphtalenetetracarboxylic dianhydride; 3) Polyvinyl chloride; 4) MCMB: Mesocarbon microbeads.

- Doeff, M. M.; Ma, Y.; Visco, S. J.; DeJonghe, L. C., Electrochemical Insertion of Sodium into Carbon. *Journal of The Electrochemical Society* **1993**, 140, (12), L169.

2. Alcántara, R.; Jiménez-Mateos, J. M.; Lavela, P.; Tirado, J. L., Carbon black: a promising electrode material for sodium-ion batteries. *Electrochemistry Communications* **2001**, 3, (11), 639-642.
3. Bommier, C.; Luo, W.; Gao, W.-Y.; Greaney, A.; Ma, S.; Ji, X., Predicting capacity of hard carbon anodes in sodium-ion batteries using porosity measurements. *Carbon* **2014**, 76, 165-174.
4. Wenzel, S.; Hara, T.; Janek, J.; Adelhelm, P., Room-temperature sodium-ion batteries: Improving the rate capability of carbon anode materials by templating strategies. *Energy & Environmental Science* **2011**, 4, (9), 3342-3345.
5. Luo, W.; Jian, Z.; Xing, Z.; Wang, W.; Bommier, C.; Lerner, M. M.; Ji, X., Electrochemically Expandable Soft Carbon as Anodes for Na-Ion Batteries. *ACS Central Science* **2015**, 1, (9), 516-522.
6. Fan, L.; Liu, Q.; Chen, S.; Xu, Z.; Lu, B., Soft Carbon as Anode for High-Performance Sodium-Based Dual Ion Full Battery. *Advanced Energy Materials* **2017**, 7, (14), 1602778.
7. Jian, Z.; Bommier, C.; Luo, L.; Li, Z.; Wang, W.; Wang, C.; Greaney, P. A.; Ji, X., Insights on the Mechanism of Na-Ion Storage in Soft Carbon Anode. *Chemistry of Materials* **2017**, 29, (5), 2314-2320.
8. Pol, V. G.; Lee, E.; Zhou, D.; Dogan, F.; Calderon-Moreno, J. M.; Johnson, C. S., Spherical Carbon as a New High-Rate Anode for Sodium-ion Batteries. *Electrochimica Acta* **2014**, 127, 61-67.
9. Li, W.; Zhou, M.; Li, H.; Wang, K.; Cheng, S.; Jiang, K., A high performance sulfur-doped disordered carbon anode for sodium ion batteries. *Energy & Environmental Science* **2015**, 8, (10), 2916-2921.
10. Stevens, D. A. Mechanisms for sodium insertion in carbon materials. 2000.
11. Stevens, D. A.; Dahn, J. R., The Mechanisms of Lithium and Sodium Insertion in Carbon Materials. *Journal of The Electrochemical Society* **2001**, 148, (8), A803-A811.
12. Bai, Y.; Wang, Z.; Wu, C.; Xu, R.; Wu, F.; Liu, Y.; Li, H.; Li, Y.; Lu, J.; Amine, K., Hard Carbon Originated from Polyvinyl Chloride Nanofibers As High-Performance Anode Material for Na-Ion Battery. *ACS Applied Materials & Interfaces* **2015**, 7, (9), 5598-5604.
13. Tang, K.; Fu, L.; White, R. J.; Yu, L.; Titirici, M.-M.; Antonietti, M.; Maier, J., Hollow Carbon Nanospheres with Superior Rate Capability for Sodium-Based Batteries. *Advanced Energy Materials* **2012**, 2, (7), 873-877.
14. Yu, L.; Song, H.; Li, Y.; Chen, Y.; Chen, X.; Zhou, J.; Ma, Z.; Wan, X.; Tian, P.; Wu, J., Rod-like Ordered Mesoporous Carbons with Various Lengths as Anode Materials for Sodium Ion Battery. *Electrochimica Acta* **2016**, 218, 285-293.
15. Alcántara, R.; Fernández Madrigal, F. J.; Lavela, P.; Tirado, J. L.; Jiménez Mateos, J. M.; Gómez de Salazar, C.; Stoyanova, R.; Zhecheva, E., Characterisation of mesocarbon microbeads (MCMB) as active electrode material in lithium and sodium cells. *Carbon* **2000**, 38, (7), 1031-1041.
16. Song, L.-J.; Liu, S.-S.; Yu, B.-J.; Wang, C.-Y.; Li, M.-W., Anode performance of mesocarbon microbeads for sodium-ion batteries. *Carbon* **2015**, 95, 972-977.
17. Cao, B.; Liu, H.; Xu, B.; Lei, Y.; Chen, X.; Song, H., Mesoporous soft carbon as an anode material for sodium ion batteries with superior rate and cycling performance. *Journal of Materials Chemistry A* **2016**, 4, (17), 6472-6478.
18. Alcántara, R.; Jiménez Mateos, J. M.; Tirado, J. L., Negative Electrodes for Lithium- and Sodium-Ion Batteries Obtained by Heat-Treatment of Petroleum Cokes below 1000°C. *Journal of The Electrochemical Society* **2002**, 149, (2), A201.
19. Zhu, H.; Shen, F.; Luo, W.; Zhu, S.; Zhao, M.; Natarajan, B.; Dai, J.; Zhou, L.; Ji, X.; Yassar, R. S.; Li, T.; Hu, L., Low temperature carbonization of cellulose nanocrystals for high performance carbon anode of sodium-ion batteries. *Nano Energy* **2017**, 33, 37-44.
20. Hou, H.; Banks, C. E.; Jing, M.; Zhang, Y.; Ji, X., Carbon Quantum Dots and Their Derivative 3D Porous Carbon Frameworks for Sodium-Ion Batteries with Ultralong Cycle Life. *Advanced Materials* **2015**, 27, (47), 7861-7866.